

## DRAFT IMECE2004-59908

### MODELING AND CHARACTERIZATION OF THE SCRATCH DRIVE ACTUATOR

Jessica R. Bronson  
Department of Mechanical and Aerospace  
Engineering, University of Florida, Gainesville, FL

James J. Allen  
Microsystem Device Technologies  
Sandia National Laboratories, Albuquerque, NM

Gloria J. Wiens  
Department of Mechanical and Aerospace  
Engineering, University of Florida, Gainesville,  
FL

#### ABSTRACT

This paper presents the characterization of scratch drive actuators (SDAs) built using Sandia National Laboratories (SNL) SUMMiT™ V micromachining process. Experimental data is used to characterize the output step size as a function of input voltage. This data is correlated to an analytical model in an effort to better understand and predict the stepping motion of these devices. The experimental results match well with the predictions from the model. Experimental data shows that the step sizes are on the order of 10 nm, and force estimates show that one plate is capable of producing forces in excess of 100  $\mu\text{N}$  for each step.

#### INTRODUCTION

Development of microactuator technology is key to the future of microelectromechanical systems (MEMS). One such actuator that has demonstrated great potential is the Scratch Drive Actuator (SDA). These devices have a compact size and can produce high forces over long distances. SDAs are electrostatically actuated and rely greatly on frictional forces to produce in-plane, stepwise motion. Because of this, the actuation method is highly nonlinear, resulting in intermittent and sometimes unpredictable operation. The ability to predict the stepwise behavior of these devices will greatly aid in future design efforts. In this paper, an analytical model that predicts the step size of the SDA as a function of the driving voltage is presented. The model is validated with experimental data from SDAs of various sizes developed in the SUMMiT™ V process at Sandia National Laboratories (SNL).

MEMS actuators such as SNL's electrostatic microengines have been shown to produce forces of 27  $\mu\text{N}$  on the drive pin

[1]; however they are limited in stroke and can be physically large structures, approximately 5 mm<sup>2</sup>, taking up valuable room on the die. The scratch drive actuator (SDA) is a compact device that demonstrates the ability to produce very large forces. One study found that a single SDA produced over 250  $\mu\text{N}$  of force over a distance of 10  $\mu\text{m}$ , and that force was increased by creating an array of four devices to obtain 850  $\mu\text{N}$  over the same range [2]. By allowing the SDA to travel further and by creating arrays of devices, these actuators are capable of achieving even higher forces in the mN range.

SDAs, first introduced by Akiyama and Shono at the University of Tokyo [3], have been used successfully for the self-assembly of micromachined MEMS by providing force for lifting structures out of plane of the substrate [4-9]. SDAs may also be arranged in a rotary array and used to drive a micro rotary fan [10,11]. Linderman conducted an in depth study of SDAs in [11]. An analytical model was derived to determine the optimal plate length to achieve minimum power consumption. In addition, devices were created in large arrays, demonstrating the advantage of being able to increase the output force. SDAs have also been implemented as precision positioning devices such as an XY stage for optical alignment [12].

The goal of this project is to characterize SDAs fabricated in Sandia National Laboratories (SNL) five-level surface micromachining process SUMMiT™ V and extract a model for these devices in order to better understand their operation and aid in future design efforts. Of particular interest is to determine the output step size as a function of the input voltage. Presented below is a description of the operating principle, fabrication, analytical model, experimental setup, results, and conclusions.

## NOMENCLATURE

$L$	= plate length
$W$	= plate width
$t$	= plate thickness
$L_B$	= bushing height
$V$	= applied voltage
$x$	= step size
$F_e$	= electrostatic force
$\epsilon$	= permittivity of dielectric
$A$	= plate area
$d$	= gap between plates
$L_D$	= length of device on substrate prior to actuation
$\phi$	= angle between bushing and substrate prior to actuation
$h$	= geometric term used in model
$m$	= geometric term used in model
$\theta$	= angle that the bushing makes during actuation
$K$	= torsional stiffness
$F$	= applied force during actuation
$F_T$	= reaction force at tail
$F_B$	= reaction force at bushing
$L_{es}$	= location of applied force $F$
$F_D$	= drag force
$\mu$	= coefficient of friction
$A_{att}$	= attached plate area
$S_r$	= sum of the square of the residuals
$SF$	= scale factor
$V_{min}$	= minimum voltage at which actuation occurs
$x_{max}$	= largest step size achieved
$V_{max}$	= lowest voltage for which largest step size is achieved

## THEORY AND OPERATING PRINCIPLE

Scratch drive actuators, shown schematically in Fig. 1, consist of a flat plate suspended above the substrate by folded spring arms. There is a short bushing projecting down from the plate. These devices are electrostatically actuated and rely greatly on frictional forces to produce in-plane linear motion. As a voltage is applied across the substrate and the plate, the plate is pulled down and the bushing flexes out, resulting in an incremental "step". This process is repeated to result in actuation over large distances. Previously published work estimates that each step is on the order of 10 nm [12].

The electrostatic force may be considered as that of a parallel plate capacitor and is given as a function of the permittivity of the dielectric,  $\epsilon$ , the area of the plate,  $A$ , the applied voltage,  $V$ , and the gap between the plates,  $d$  [13].

$$F_e = -\frac{\epsilon AV^2}{2d^2} \quad (1)$$

From equation (1) it is clear that electrostatic force is always attractive regardless of the polarity of the voltage signal.

Once the plates are actuated, they do not appear to return to their original position; rather the free end of the plate tends to remain down on the substrate. This could be the result of

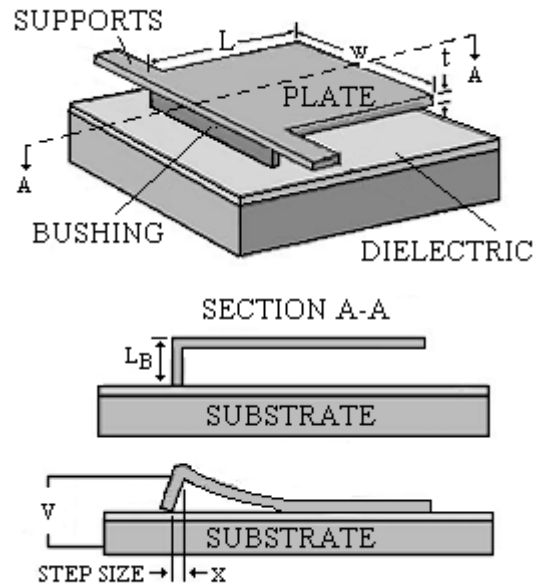


**Fig. 1. Schematic of Scratch Drive Actuator (SDA) and cross-sectional representation of operation.**

stiction, dielectric charge trapping, or a combination of factors. Because of this, as the SDA is driven, it must, in effect, drag this attached tail along. Linderman suggests in [11] that because of this phenomenon, there is an optimal plate length in order to achieve the most efficient device in terms of power consumption. If a plate is too long, it cannot overcome the drag force, but if it is too short, the actuation voltage is too high [11].

A question still unanswered is that of what appropriate drive signal to use to optimize the performance of the SDA. Different authors have employed different drive signals. Akiyama, *et al.* used a pulse waveform of a given amplitude to operate the SDAs [3,14]. In another case, a triangular wave is used [12]. In [11], Linderman suggests that because of the drag caused by the attached area, it is best to operate the SDAs with a dc-offset that corresponds to the voltage it takes to pull the tip of the suspended plate to the substrate. This concept is investigated here.

## DEVICE FABRICATION

The SDAs were fabricated using the SUMMiT™ V process at Sandia National Laboratories. The process flow diagram is given in Fig. 2. The substrate is <100> n-type silicon, the structural layer is polysilicon and silicon dioxide is used as a sacrificial layer. The substrate is covered in 0.8  $\mu\text{m}$  of thermal oxide and then 0.6  $\mu\text{m}$  of silicon nitride to protect the oxide and provide electrical and thermal isolation. The released structure is suspended above the substrate 0.5  $\mu\text{m}$  by the supports. These supports are better seen in the SEM

photograph of the fabricated devices in Fig. 2. The plate is 2.5  $\mu\text{m}$  thick and the bushing is 0.5  $\mu\text{m}$  long.

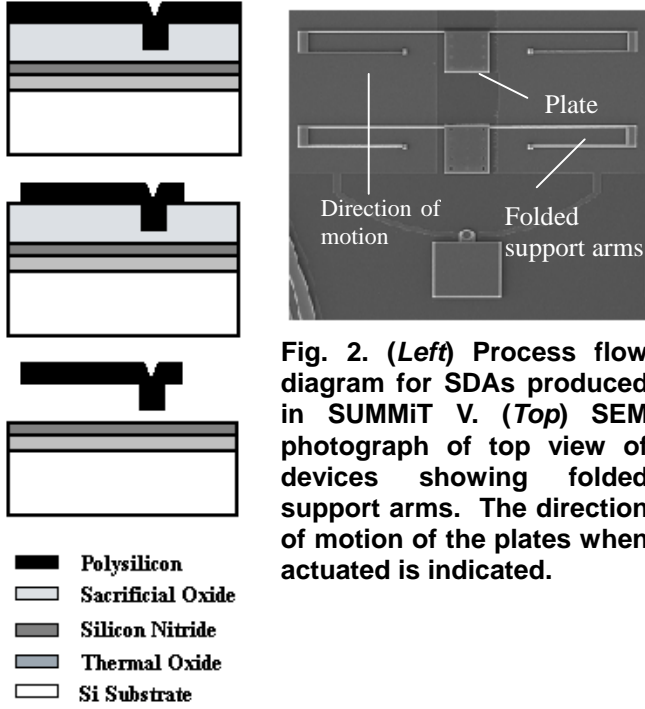


Fig. 2. (Left) Process flow diagram for SDAs produced in SUMMiT V. (Top) SEM photograph of top view of devices showing folded support arms. The direction of motion of the plates when actuated is indicated.

two rigid plates and treating the electrostatic force as a point load,  $F$ , a relationship between step size,  $x$ , and voltage,  $V$ , is obtained. In reality, the plate of the SDA will not remain rigid, but rather it will flex as shown schematically in Fig. 1. In addition, the electrostatic force will actually be distributed over the plate. However, these assumptions allow for a simplified analysis. Before this analysis can continue it is necessary to define several geometric terms illustrated in Fig. 3.

$L$  is the length of the plate and  $L_B$  is the height of the bushing. Prior to actuation, the plate and bushing are assumed to be at  $90^\circ$ , and the projected length of the entire structure on the substrate  $L_D$  is given as a result of Pythagorean's theorem.

$$L_D = \sqrt{L^2 + L_B^2} \quad (2)$$

The angle  $\phi$ , shown in Fig. 3(a) is

$$\phi = \sin^{-1}\left(\frac{L}{L_D}\right) \quad (3)$$

and two additional terms,  $h$  and  $m$  are

$$h = L_B \sin \phi \quad (4)$$

$$m = L_B \cos \phi \quad (5)$$

Once a force is applied, the bushing will deflect an angle  $\theta$  that may be estimated as

$$\theta = \frac{xL_D}{L_B L} \quad (6)$$

As the bushing deflects, a restoring moment acts on the structure that is a function of the torsional stiffness of the L-shaped beam, and of the folded support arms,  $K$ . The vertical reaction forces,  $F_T$  and  $F_B$  are functions of the electrostatic force,  $F$ , that is treated as a point load located a distance  $L_{es}$  from the tail of the plate.  $\epsilon$  is the permittivity of the gap, and  $W$  is the plate width.

$$F = \frac{-\epsilon W (L_D - m) V^2}{2h^2} \quad (7)$$

$$F_T = F \left( \frac{L_D - L_{es} + x}{L_D + x} \right) \quad (8)$$

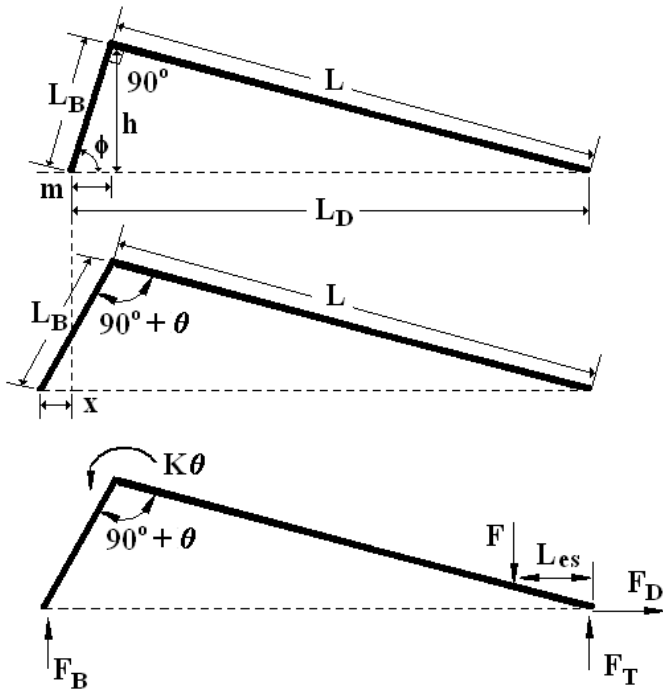


Fig. 3. Model nomenclature

## MODELING

An elementary, static analysis is used to determine the fundamental equations of motion. By considering the SDA as

$$F_B = F \left( \frac{L_{es}}{L_D + x} \right) \quad (9)$$

The friction produced by the attached end of the plate is assumed to act as Coulomb friction and is included as a force  $F_D$ . It can be modeled as a product of the coefficient of friction between the polysilicon plate and the nitride,  $\mu$ , and the electrostatic normal force caused by the attached area of plate,  $A_{att}$ .

$$F_D = \mu F_e = \mu \left( \frac{\epsilon A_{att} V^2}{2d^2} \right) = DV^2 \quad (10)$$

Recall from equation (1) that the electrostatic normal force is a function of the gap,  $d$ , in this case given by the thickness of the insulating nitride and oxide layers. The permittivity,  $\epsilon$  is the equivalent permittivity of the two insulating layers. The friction force is also a function of the voltage,  $V$ , and the other terms in equation (10) may be considered as an unknown drag coefficient,  $D$ , that may be determined by fitting the model to experimental data.

Therefore  $D$  can be represented as

$$D = \frac{\mu \epsilon A_{att}}{2d^2} \quad (11)$$

Finally, by finding the sum of the static moments of all the forces described above, the following relationship for step size  $x$  can be derived.

$$x = \frac{(2FL_{es}(L_D - m) - DV^2 h L_D) L_B L}{KL_D^2 + (DV^2 h + 4FL_{es}) L_B L} \quad (12)$$

Equation (13) contains many terms that are a product of the geometry of the device, but it is essentially a function of the applied voltage and the drag coefficient.

In order to determine a value for  $D$ , it is necessary to perform a nonlinear least-squares fit on experimental data. This method will find the best value for the unknown parameters, in this case,  $D$ , such that the resulting sum of the square of the residuals,  $S_r$ , is minimized.  $S_r$  is found by subtracting the true estimated value of step size that is a function of  $D$  and  $V_i$ ,  $x_i(D, V_i)$ , from the true value determined experimentally,  $x_{true}$ . This value is squared and summed for all  $n$  data points [15].

$$S_r = \sum_{i=1}^n [x_{true,i} - x_i(D, V_i)]^2 \quad (14)$$

The values of  $D$  determined here may be used in conjunction with published values for friction to estimate the attached area of the plate. Conversely, experiments may be performed to estimate the attached area, and then the friction coefficient or  $D$  may be estimated in turn.

## EXPERIMENTAL SETUP

Figure 4 depicts the equipment setup for the characterization of the SDAs. The drive signal is sent from the computer to Sandia's custom built amplifier and then to the device on a probe station. The motion of the SDA is captured with a high-speed camera and transmitted back to the computer where the image is processed using Sandia's MEMscript software. This software uses image recognition algorithms to track the forward motion of the SDA.

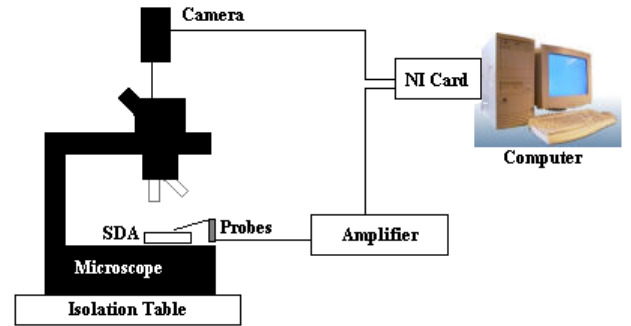


Fig. 4. Experimental setup

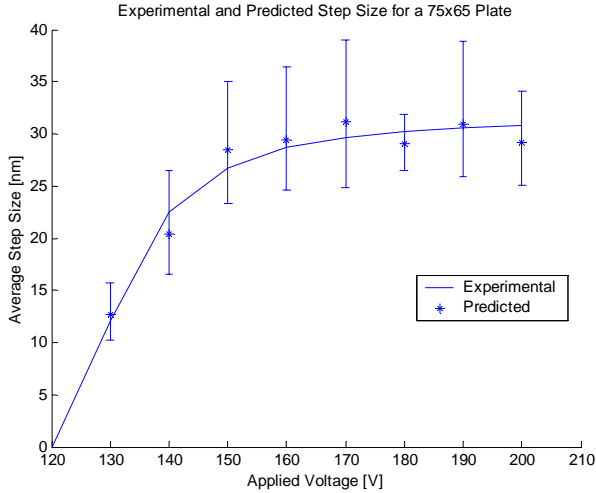
For the experiment, there are two sets of SDAs being considered. One set is 75  $\mu\text{m}$  wide and the other is 200  $\mu\text{m}$  wide. Both sets have plates of varying lengths, 65, 75, 85, 95  $\mu\text{m}$ . The devices are operated using a sinusoidal input with different amplitudes. The frequency of the signal is a constant 100 Hz. As each individual step size is very small, on the order of ten nanometers, it is difficult to detect each individual step. Therefore, data is collected over 600 steps and then an average step size is calculated.

## RESULTS AND DISCUSSION

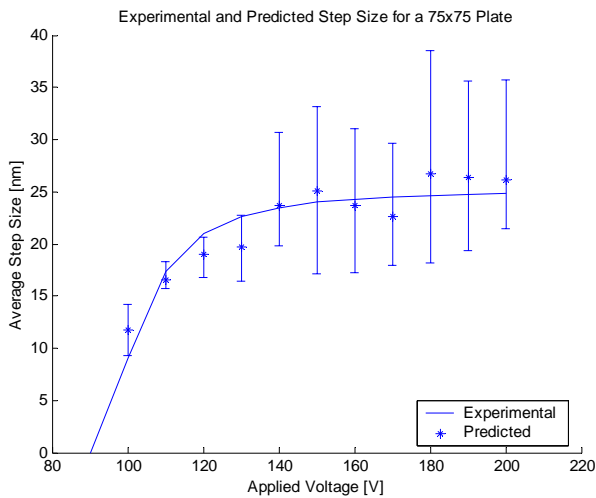
Based on the analytical model in equation (12), a least-squares curve fit was performed using the 'lsqcurvefit' command in MATLAB<sup>®</sup>. Preliminary results from the model proved to be several times larger than those determined experimentally. Therefore, the predicted results were reduced by a scale factor, SF, such that the right hand side of equation (13) is multiplied by  $SF^{-1}$ . The need for this scale factor can be attributed to the simplistic geometric assumptions made in the model. The variables to be estimated by the least squares fit are  $D$ , and SF.

Figures 5 and 6 show plots of the experimental data and the predicted model for SDAs with plate sizes 75  $\mu\text{m}$  wide. Figures 7 and 8 show the results for plates 200  $\mu\text{m}$  wide. The data plotted is an average for multiple tests of devices from

different die at the same voltages. Error bars indicate the maximum and minimum values obtained. It can be seen that the step size measurements can vary substantially. This, in part, can be attributed to variations from devices on different die.

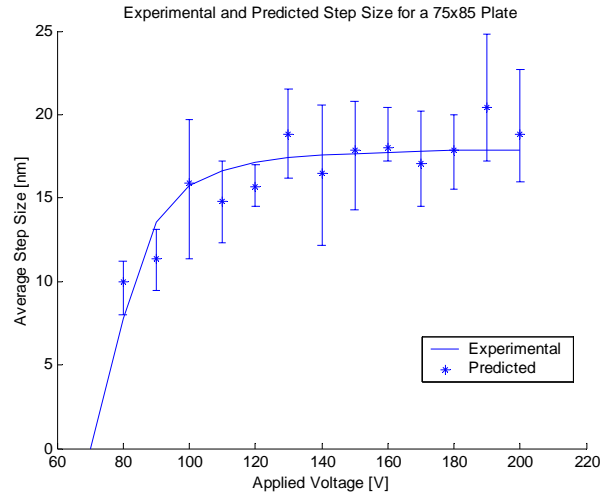


(a)

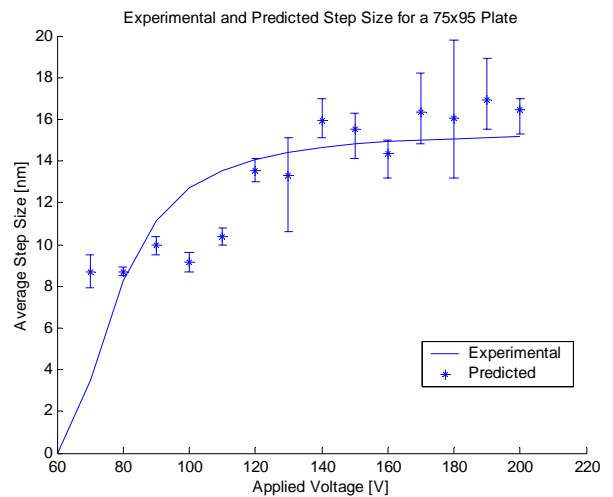


(b)

The force output may be determined from the experimental data if the linear spring stiffness of the support arms is known. Through classical beam mechanics, the stiffness is determined to be 3.77 N/m. The force output for these devices ranges from 60  $\mu\text{N}$  for longer plate lengths, to 110  $\mu\text{N}$



(c)



(d)

**Fig. 5. Plots showing the experimental and predicted step size of the SDA for a given voltage for plates of dimensions: (a) 65x75, and (b) 75x75  $\mu\text{m}^2$ .**

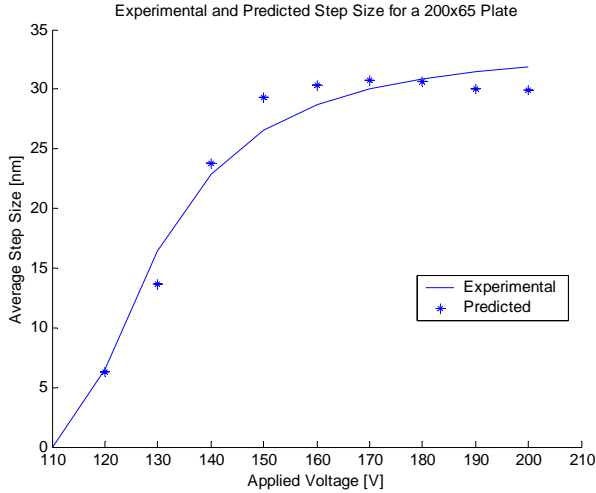
**Fig. 6. Plots showing the experimental and predicted step size of the SDA for a given voltage for plates of dimensions: (c) 85x75, and (d) 95x75  $\mu\text{m}^2$ .**

There is a voltage at which the SDAs begin to actuate,  $V_{\min}$ . Voltages below  $V_{\min}$  will not cause actuation. From the plots it appears that at higher voltages, the curve begins to flatten such that you can approximate the lowest voltage,  $V_{\max}$ , for which the largest step size,  $x_{\max}$ , may be achieved. This  $V_{\max}$  is useful to determine the power requirements of the system. Table 1 summarizes the values  $D$ ,  $SF$ ,  $S_s$ ,  $V_{\min}$ ,  $x_{\max}$ , and  $V_{\max}$  for all the plate sizes studied.

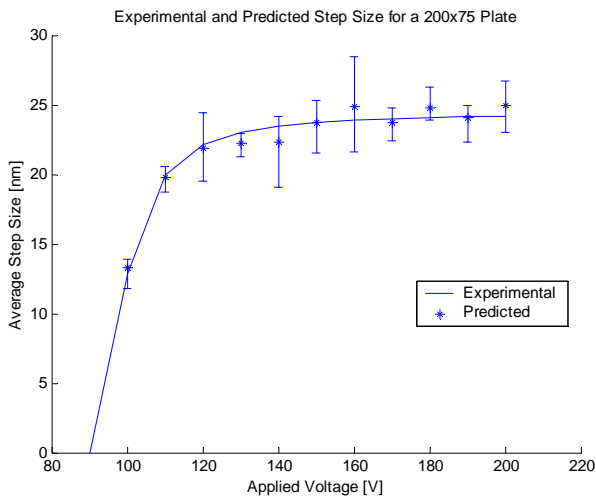
for shorter plates. Results for the 75  $\mu\text{m}$  wide plates and the 200  $\mu\text{m}$  wide plates are shown in Fig. 7 and 8, respectively. These values are similar to published values of force measurements [2]. It is logical that the shorter, stiffer plates would provide more force, but the trade off is a higher actuation voltage and  $V_{\min}$ .

In addition to the results presented above, Linderman's concept of conserving power by driving the

device with a dc offset was considered. The dc offset may be determined experimentally by increasing a dc voltage on the plates until the free end is pulled down to the substrate. This occurs very abruptly as the plates ‘snap’ down to the surface and is easily observed using optical interferometry. However, using these



(a)



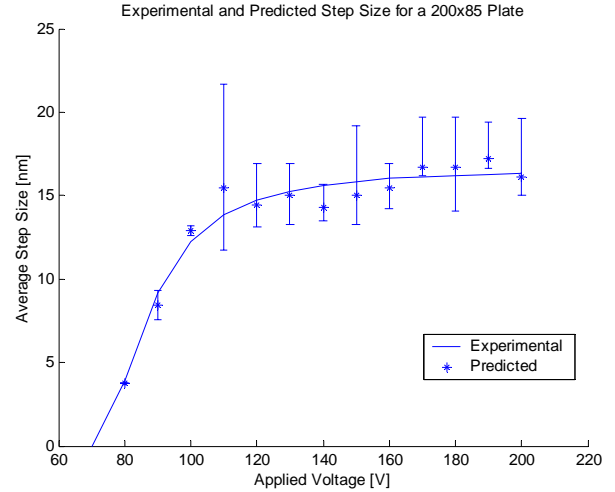
(b)

**Fig. 6. Plots showing the experimental and predicted step size of the SDA for a given voltage for plates of dimensions: (a) 65x200, and (b) 75x200  $\mu\text{m}^2$ .**

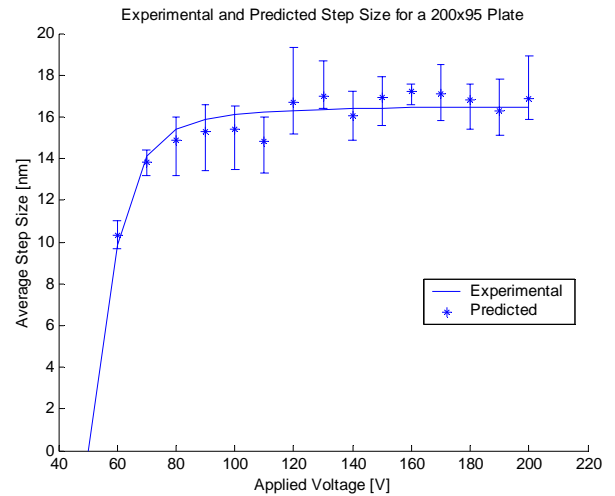
**Table 1. A summary of the results from the least squares fit of the model to the experimental data.**

Plate Size ( $\mu\text{m}^2$ )	D	SF	$S_r$	$V_{act}$ (V)	$x_{max}$ (nm)	$V_{min}$ (V)
65x75	0.0721	2.0600	14.701	130	30	160
75x75	0.0741	2.9801	35.022	100	25	150
85x75	0.1128	4.7119	26.550	80	18	130

95x75	0.0478	6.1539	63.284	70	16	120
65x200	0.0279	1.9401	24.686	120	30	160
75x200	0.1489	3.0813	4.4102	100	25	130
85x200	0.0461	5.1065	7.8558	70	17	140
95x200	0.2453	5.7447	5.4488	60	16	90



(c)



(d)

**Fig. 7. Plots showing the experimental and predicted step size of the SDA for a given voltage for plates of dimensions: (a) 85x200, and (b) 95x200  $\mu\text{m}^2$ .**

results to provide a dc offset to the drive signal produced inconclusive results as to the effect this had on the step size.

## CONCLUSIONS AND FUTURE WORK

Presented here is the characterization and analytical model to predict the step size as a function of input voltage for scratch drive actuators. The model produced results that must be scaled to fit the data. This discrepancy can be attributed to the assumptions made in modeling that the plate remains rigid during actuation and that the electrostatic force acts at only

point. The model also relies on a frictional drag term,  $D$ , that is a function of the attached area of the plate. This term and the scale factor for the model are determined through least squares curve fitting.

The plates produce step sizes on the order of 10 nm and

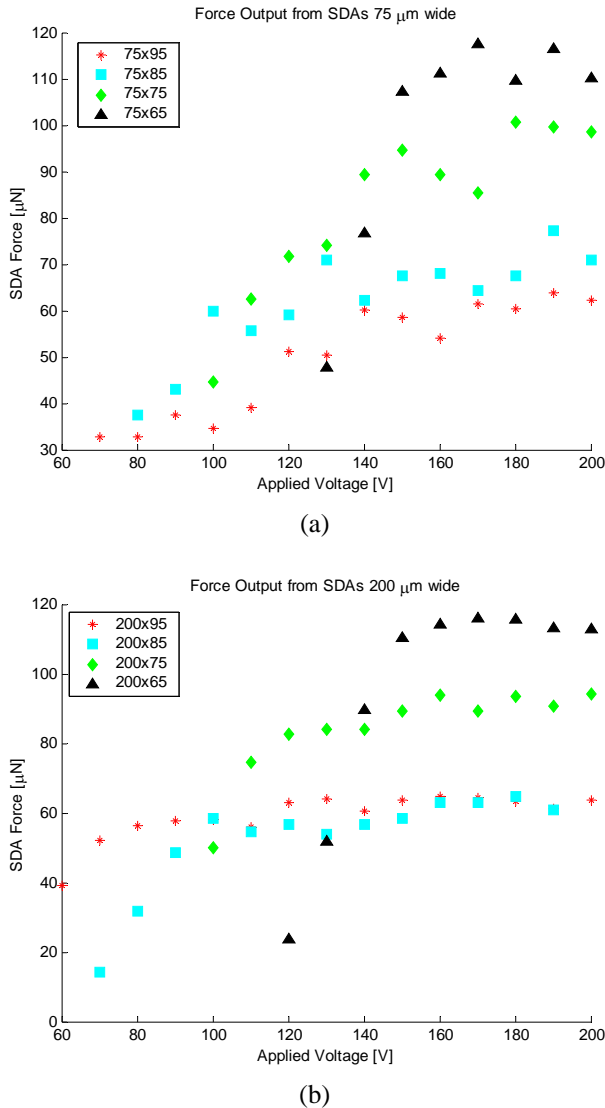


**Fig. 9. Force produces for one step size for SDAs (a) 75  $\mu\text{m}$  wide, and (b) 200  $\mu\text{m}$  wide. These data points are calculated directly from the step size data.**

output forces of over 110  $\mu\text{N}$  for one step size. It has been found that shorter plates are able to produce larger step sizes and forces than the longer plates, but require larger minimum voltages.

Future work includes further verification of the analytical model for SDAs of different plate thickness and bushing height. Another issue that deserves attention is determining an optimal drive signal and more investigation into the effects of using a dc offset voltage. This will lead to development of more

complex micro devices that utilize the small size and large forces produced by the SDA. In addition, a more versatile bi-directional device is being developed.

## ACKNOWLEDGMENTS

This work was supported by the United States Department of Energy under Contract DE-AC04-94AL85000. Sandia is a multiprogram laboratory operated by Sandia Corporation, a Lockheed Martin Company, for the United States Department of Energy.

## REFERENCES

- [1] E. Pryputniewicz, S. Miller, M. de Boer, G. Brown, R. Biederman, and R. Pryputniewicz, "Experimental and analytical characterization of dynamic effects in electrostatic microengines," *Proc. Internat. Symp. on Microscale Systems*, Orlando, FL, 4 June 2000, pp. 80-83.
- [2] L. Li, J. Brown, and D. Uttamchandani, "Study of scratch drive actuator force characteristics," *J. Micromech. Microeng.*, vol. 12, p. 736, 2002.
- [3] T. Akiyama, and K. Shono, "Controlled stepwise motion in polysilicon microstructures," *J. Microelectromechanical Systems*, vol. 2, no. 3, p. 106, 1993.
- [4] T. Akiyama, D. Collard, and H. Fujita, "Scratch drive actuator with mechanical links for self-assembly of three-dimensional MEMS", *J. Microelectromechanical Systems*, vol. 6, no. 1, p. 10, 1997.
- [5] S-S. Lee, L-S Huang, C-J Kim, and M. Wu, "Free-space fiber-optic switches based on MEMS vertical torsion mirrors," *J. Lightwave Tech.*, vol. 17, no. 1, p. 7, 1999.
- [6] E. Quevy, P. Bigotte, D. Collard, and L. Buchailot, "Large stroke applications of continuous membrane for adaptive optics by 3D self-assembled microplates," *Sensors and Actuators A*, vol. 95, p. 183, 2002.
- [7] L. Y. Lin, J. L. Shen, S. S. Lee, M. C. Wu, "Surface-Micromachined Micro-XYZ Stages for Free-Space Microoptical Bench," *IEEE Photonics Tech. Letters*, vol. 9, no. 3, pp. 345-347, Mar. 1997.
- [8] L. Fan, M. Wu, K. Choquette, M. Crawford, "Self-Assembled Microactuated XYZ stages for Optical Scanning and Alignment," *1997 Intl. Conf. On Solid-State Sensors and Actuators, Transducers '97, Chicago, June 16-19, 1997*, p. 319.
- [9] L. Fan, S. Lee, M. Wu, "Self-Assembled Microactuated XYZ stages for Optical Scanning and Alignment," *Lasers and Electro-Optics Society Annual Meeting, 1997. LEOS '97 10<sup>th</sup> Annual Meeting. Conf. Proc., IEEE*, vol. 1, pp. 266-267, 1996.
- [10] R. Linderman, P. Kladitis, V. Bright, "Development of the micro rotary fan," *Sensors and Actuators A*, vol. 95, p. 135, 2002.
- [11] R.J. Linderman, "Development of the scratch drive actuator motor," *Master's Thesis*, University of Colorado, Boulder, CO, 2000.

- [12] P. Langlet, D. Collard, T. Akiyama, and H. Fujita, "A quantitative analysis of scratch drive actuation for integrated X/Y motion," 1997 *Int. Conf. on Solid-State Sensors and Actuators., Transducers '97, Chicago, June 16-19, 1997*, p. 773.
- [13] S. Senturia, *Microsystem Design*, Second printing Kluwer Academic Publishers, Boston, 2001.
- [14] T. Akiyama, and H. Fujita, "A quantitative analysis of scratch drive actuator using buckling motion," *Microelectromechanical Systems, 1995, MEMS '95, Proc. IEEE*, p. 310, 1995.
- [15] S. Chapra, and R. Canale, *Numerical Methods for Engineers*, 4<sup>th</sup> ed., McGraw Hill, 2002.